Sediment-encased pressure-temperature maturation experiments chemically simulate natural diagenesis of melanin

Arindam Roy
University of Hong Kong https://orcid.org/0000-0002-4890-6851
Michael Pittman (mpittman@hku.hk)
The University of Hong Kong https://orcid.org/0000-0002-6149-3078
Thomas Kaye
Foundation for Scientific Advancement https://orcid.org/0000-0001-7996-618X
Evan Saitta
Field Museum of Natural History https://orcid.org/0000-0002-9306-9060

Article

Keywords: palaeocolour reconstruction, fossil melanin, diagenesis, mass spectrometry, experimental taphonomy

Posted Date: December 11th, 2020

DOI: https://doi.org/10.21203/rs.3.rs-106894/v1

Abstract

Palaeocolour informs the ecology, physiology and behaviour of extinct animals. However, there is room for improvement in palaeocolour reconstructions due to poor understanding of the chemical changes occurring in pigmented soft tissues during fossilisation. Pressure-temperature maturation experiments are key to expanding our knowledge of pigmented soft-tissue preservation. Prior work on melanin has yielded limited insights in highly closed systems due to stable and volatile diagenetic products mixing and obscuring chemical analyses as well as in open systems because of the leaking and loss of samples. To replicate natural fossilisation, modern melanised feathers were encased in a porous bentonite clay matrix and subjected to a next-generation maturation system. Resultant samples closely resemble natural fossils both visually and chemically. Using mass spectrometry, increased crosslinking is identified within the overall melanin polymer alongside predictable loss of volatile nitrogen/sulphur bearing molecular groups with higher maturation temperatures for the first time, chemically simulating natural melanin diagenesis.

Introduction

Experiments within a laboratory setting have played pivotal roles in disentangling taphonomic variables, particularly as they relate to palaeocolour reconstruction[1, 2, 3]. The bulk of the fossil record consists of biomineralised hard tissues such as shells or skeletal material (e.g., bones and teeth) whereas, occasionally, soft tissues (e.g., skin [4] , feathers[5, 6, 7], scales [8], muscles[9, 10], visceral organs[2, 11], eyes[12], claw sheaths[8], hair[13, 14], and embryos[15]) are preserved with relatively high anatomical (macro- and microscopic) and/or biomolecular fidelity, offering unique insights into the biology of extinct organisms. Exceptional preservation of soft tissues occurs when the dead organism passes several physical and biochemical taphonomic filters that results in selective removal, transformation, or preservation of anatomy and biomolecules[16, 17, 18]. Efforts in palaeocolour research therefore, must take into account the effects of diagenetic maturation on organic staining, melanosome shapes, and melanin chemistry [3, 13, 19] so as to achieve higher precision in articulating ecological, physiological, and behavioural hypotheses. Models of exceptional preservation developed from experiments in controlled laboratory settings benefit from the ability of researchers to focus tests on specific taphonomic variables of interest and to control many potentially confounding ones. Experimental taphonomy has focused on simulating key aspects of exceptional preservation: (1) pre-burial transport [20, 21, 22], (2) pre-burial decay[18, 23, 24], (3) diagenesis (i.e., post-burial effects of heat and pressure over long periods)[13, 25, 26], and (4) pre- and post-burial, microbially mediated authigenic mineralisation[9, 15, 27].

The earliest record of fossil melanin pigments goes back to ~300 million years ago[12]. Therefore, exceptionally preserved melanin for many fossils has undergone prolonged heat and pressure-mediated diagenesis for the life of its burial. Artificial maturation experiments to simulate late diagenesis usually subject melanised soft tissues to elevated pressure (e.g., P:~250 bars) and temperature (e.g. T:~45–300 °C) for comparatively short durations (e.g., hours–days) [3, 13, 26, 28, 29]. The rationale for these treatments is largely based on chemical kinetics wherein elevated temperature increases the rate of degradative reactions such that long-term diagenesis under relatively ‘long time, cooler geothermal conditions’ can be approximated under timescales amenable for laboratory experiments. Typically, P/T maturation experiments have been conducted through three different methods: (1) closed-system capsule maturation[13], (2) open-system foil maturation[3], and (3) sediment-encased maturation[28] (**Table 1**). Closed system maturation involves sealing tissue samples inside tiny Au/Ag capsules (~2 mm diameter) that are welded shut and placing them inside water-pressurised autoclaves. In contrast, tissues of larger sizes have been wrapped in aluminium foil, a highly open system, and subjected to heat and pressure in Ar-gas-pressurised autoclaves, but samples have been known to completely leak out of foil, leading to irretrievable products[29, 30]. These setups represent unnatural extremes in closed vs. open system dynamics, with the former trapping labile, mobile, and volatile products alongside more stable, immobile products predicted to survive diagenesis. Furthermore, both have difficulty linking chemical changes to changes in anatomical preservation since the methods require the extrusion of products out of the capsule/foil, leading to loss or alteration of anatomical details. Additionally, capsule maturation can trap transformed products normally dissipated in natural fossilisation, which can obscure the signals of recalcitrant components.

Table 1. Capsule versus sediment-encased P/T maturation

	Capsule Maturation	Sediment-encased Maturation
Sample Placement	· Sealed inside inert metal capsules (i.e., totally closed system).	· Encased within a compacted, porous sediment matrix (i.e., selectively open system).
Sample Size	· Capsule diameter <2 mm. · Larger samples have alternatively been wrapped in aluminium foil and put into Ar gas-pressurised autoclaves, but the system becomes totally open.	· Tissue samples of up to 10–15 mm diameter encased in sediment matrix.
P/T Treatment	· Inside a water-pressurised autoclave. · Al-foil maturation conducted inside Ar-gas powered autoclaves	· Inside an insulated metal chamber with a heating unit (resistor coil/rod) under self-regulated compressed air. · Next-generation design of P/T maturation rig updated from the original study of Saitta *et al.*[28].
Changes in Appearance	· Often obscured by non-eliminated labile products or altered upon extraction from capsule.	· More easily studied due to easy exposure of the sample through splitting of compacted sediment. · Stable products are retained within the sediment.
System Openness	· Sealed capsule traps both labile and recalcitrant molecules produced during maturation. · Non-polar organic solvents[55] can be used to selectively recover recalcitrant molecules of low solubility but are unrealistic of natural conditions and might lead to dissolution and loss of many geochemically relevant compounds (e.g., small aliphatic lipids and sterols).	· Porous matrix allows for the filtration of labile, mobile, and volatile molecules produced during maturation, while recalcitrant molecules retained in a manner more closely approximating natural fossilisation conditions.

Capsule P/T treatments on different melanin types from feathers (black, brown, iridescent, and grey) have revealed that melanosomes undergo isometric shrinkage of about ~10–20 % due to dehydration and loss of volatile organic components[13, 23]. Chemical changes to melanin during artificial and natural maturation have been studied by comparing mass spectra of experimentally matured samples with those of fossils[13, 23, 31, 32, 33, 34]. Colleary, Dolocan [13] demonstrated through time-of-flight secondary ion mass spectrometry (ToF-SIMS) and subsequent principal components analysis (PCA) that chemical signatures of tissue-extracted melanin under closed-system, capsule maturation show a coherent pattern in which maturation leads to increased similarity to fossil samples. Thus, their experimental samples help to bridge the gap between the chemical composition of modern, unmatured melanin and fossil melanin. However, Colleary, Dolocan [13] did not provide a detailed commentary of the steps involving the chemical transformation of melanin during maturation. In addition, their chemical signatures derived from a combination of labile and recalcitrant molecular fragments trapped within the capsules. Therefore, mass spectra of experimental samples contained moieties that would otherwise have been lost in naturalistic settings. In their capsule maturation study, melanin was first extracted using the protocol outlined in Hong, Garguilo [35] and other subsequent studies[13, 36].

Sediment-encased maturation allows for a more natural approach by embedding whole melanised tissues in sediment. Saitta, Kaye [28] predicted that sediment-encased maturation of melanised tissues provides a selective filter to separate labile from stable compounds in a more naturalistic simulation. Their sediment matured samples showed volume loss of tissues, exposed melanosomes on the sediment, and the production of a dark stains from soft tissues while bones persisted. Proteinaceous and fatty tissue morphologies appeared to have been lost. Their results were consistent with capsule maturation showing keratin protein instability[32] and melanin stability[13], as well as direct analyses of fossil tissues that lack keratin protein[37] and/or consist of exposed melanosomes [38, 39]. However, the processes underlying these observations have yet to be examined at the chemical level, which is one of the goals of this study.

This study into experimental maturation and thermobaric diagenesis of melanin focuses on (1) comparing chemical changes under closed-system versus sediment-encased maturation, (2) comparing the chemistry of melanin in experimentally treated samples to exceptionally preserved fossils, (3) comparing the relative stability of phaeomelanin versus eumelanin under increasing maturation temperature to test if phaeomelanin is diagenetically less stable than eumelanin, and (4) modelling the diagenetic steps that melanin-bearing integumentary tissues take to undergo fossilisation. We examine these topics through hydraulic compaction of modern melanised feathers (black, iridescent, grey, and reddish-brown) in Ca^{2+}-bentonite clay followed by artificial P/T maturation (250 bars; approximately 190, 200, 225, 250, and 300°C) using a specialised system[28]. While the lower bound of the temperature range is based on prior work by Colleary, Dolocan [13] and McNamara, Briggs [3], the upper bound is based on measurements from some high pressure-high temperature oil wells illustrating that even relatively hot treatments (e.g., ~250–300 °C) are within the scope of natural conditions to which some fossil organic material can be exposed[26, 40, 41, 42]. Prior work simulating metamorphism[43], catagenesis, and metagenesis[44] also informs upon the chosen upper temperature bound. We then investigate the changes in macroscopic appearance of feather samples after sediment-encased maturation with increasingly higher temperatures and compare them to fossils to help judge if the colour of the stains in fossils correlate to different stages of diagenesis. Finally, we compare the chemical signature (i.e., ToF-SIMS spectra) of sediment-matured feathers to data from Colleary, Dolocan [13]and Clements, Dolocan [31] of freshly extracted melanin, capsule-matured extracted melanin (200°C and 250°C), and fossil melanised tissues. Fifty-five characteristic peaks of melanin from published literature[13, 31, 33, 34] were examined using PCA[48, 49]. This dataset comprises a diverse sampling across geological age (313–20.4 Ma, as well as extant), globally distributed fossil lagerstätten, tissue types (i.e., ink sacs, skin, feathers, hairs, eyes, and visceral organs), original colours (black, iridescent, brown, and grey; statistically/chemically predicted for fossils in the literature[13]), melanin type (eumelanin, phaeomelanin, and mixed), and invertebrate and vertebrate taxa (see **Supplementary Table S1** for details on sampling/age/locality). Our main goals in this study are to investigate if (a)

sediment-encased maturation leads to chemical filtration as hypothesised by Saitta *et al.*[31], (b) this experiment tracks melanin diagenesis, and (c) do different melanin types vary in their diagenetic stability?

Results

Physical appearance of sediment-matured feathers

All samples underwent significant volume loss after maturation. The feather sub-samples appear as organic stains and negative impressions in the matrix (**Fig. 1**). All colour categories (black, brown, iridescent, and grey) converge as brown stains under maturation at lower temperatures of ~190–225°C . Both grey and reddish-brown feathers might show early signs of loss of organic staining at ~250°C in the form of lightening. By ~300°C, all samples lose signs of visible, dark organic stains with the product largely consisting of negative impressions of the feather structures (i.e., void spaces) in the clay matrix.

PCA of ToF-SIMS spectra from fresh, fossil, and experimentally matured samples

The first two principal components explain a total variance of 44.6% (PC1: 31.6 %, PC2: 12.6 %) (**Fig. 2a**). PCA shows that different temperature and maturation system categories (unmatured modern melanin extracts, capsule-matured melanin extracts, and sediment-matured feathers) show an ordered alignment along PC1. PC1 is heavily loaded in most part by non-hydrocarbon fragments **(Fig. 3a)**, especially N-bearing and other heteroatom-bearing fragments (C_xS_y–, C_xH_yS–, C_xN–, C_xH_yN–, C_xNS–, C_xNO–, C_xNSO–), with certain small mass fragments negatively loading the axis, while large mass fragments positively load the axis **(Fig. 3b)**. Unmatured modern melanin extracts have the lowest PC1 scores and are enriched in certain small fragments, including N- and S-bearing fragments. The capsule-matured 200 and 250°C melanin extracts appear to show increasing PC1 values with increasing temperature, indicating a slight decrease in these certain small fragments and an increase in large N/S-bearing fragments. Lower temperature sediment-matured feathers (~190°C, ~200°C, ~225°C) tend to have higher PC1 scores than capsule-matured melanin extracts at similar/equivalent temperatures, indicating depletion in those certain small fragments.

Relatively higher temperature sediment-matured feathers (~250°C) have higher PC1 scores than lower temperature regimes, indicating enrichment in large N/S fragments. The ~300°C sediment-matured feathers, however, break the observed trend of higher temperatures tending towards larger PC1 scores and appear to revert back to the PC1 origin, consistent with a loss of organic carbon.

Within each temperature and sample category (i.e., unmatured extract, capsule-matured extract, fossils, and sediment-matured feathers), it seems that high eumelanin concentration tends to have lower PC1 scores than high phaeomelanin concentration **(Fig. 2b)**, with grey and non-integumentary mixed (eu- and phaeomelanin) samples from visceral organs (eye, liver, etc.) as intermediate. This trend appears to be reversed in the ~300°C sediment-matured feathers. PC2 is heavily negatively loaded by hydrocarbon (C_xH_y–) fragments **(Fig. 3a)**. While fossil samples have PC1 values spanning from those of capsule-matured melanin extracts (200°C, 250°C) to those of lower temperature sediment-matured feathers (~190°C, ~200°C, ~225°C), they have higher PC2 values than all of the unmatured modern and experimental samples, indicating lower hydrocarbon content in fossils. Unlike many of the hydrocarbon fragments, carbon skeletons (C_n–) do not as obviously load PC2 to the exclusion of PC1. Loadings of fragments for PC1-PC4 are shown **(Supplementary Fig. S2)** and the values are tabulated **(Supplementary Table S2)**.

Discussion

Sediment-encased P/T maturation shows macroscopic staining in fossil feathers is driven by melanin

These experiments show that sediment-matured samples are highly comparable to carbonaceous compression fossils from various lagerstätten in terms of appearance and chemistry. Such macroscopic carbonaceous stains inform pigmentation and patterning in fossil taxa (e.g. stripes, mottling, bars, bandit masks, countershading)[5, 46, 47].

All feathers in these sediment-based experiments, irrespective of initial colour, leave behind brown stains on the bentonite matrix after P/T maturation. The staining appears most intense in the ~190–225°C treatments and completely disappears at ~300°C, leaving behind mainly impressions. The lower temperatures yield samples that resemble fossil feathers from the Mesozoic Altmühltal Formation[48], Crato Formation[5, 49], Jehol Group[6, 46, 47] and Koonwarra fossil beds[50] , Cenozoic Green River Formation[51] and Fur Formation[52] and many other konservat lagerstätten. However, sediment-matured iridescent feathers leave brown stains on the matrix and do not resemble the highly iridescent fossil feather (SMF ME 3850)[53] from the Eocene of Messel Formation, although this type of original iridescence retention is admittedly rare in fossils[53]. Simultaneous unidirectional compaction and P/T maturation would likely be required to preserve original alignment of melanosome layers in order to preserve iridescence in stains.

A significant body of prior evidence aligns against preservation of endogenous proteins in carbonaceous compression fossils. Saitta, Kaye [28] showed that sediment-matured samples lose protein components (evidenced by volume loss of feathers/carcasses) and retain exposed melanosomes on the sediment matrix. This pattern is also noted in fossils[5, 6], for example, where only darkly stained striped sections of feathers preserve melanosome films, whereas unpigmented sections show only sediment matrix without any proteinaceous ultrastructural features. Therefore, if proteins were to survive (relatively intact or cross-linked with sugars or lipids) organic mass in the feather tissue would not be significantly lost and melanosomes would be obscured by these polymers[54]. Total ion pyrochromatograms by both Saitta, Rogers [29] and Cincotta, Nguyen Tu [55] showed a lack of enriched peaks resulting from the pyrolysis of modern feather protein in both P/T-matured and fossil samples. ToF-SIMS spectra of experimental samples and fossils are

quite different from
α/β-keratin controls from Schweitzer, Zheng [56] **(Supplementary Fig. S3)**.

An alternative view[57] suggests that brown stains in fossils can be readily produced by remnant proteinaceous components oxidatively condensing with sugar/lipid moieties to yield N-linked melanoidin-like heterocyclic polymers (i.e., advanced glycation end products [AGE] and advanced lipooxidation end products [ALE]). Wiemann, Fabbri [58] conducted their experiments at low temperatures (45–120°C) for short durations (10 mins–1hr) and did not elevate pressure. Vapourisation and removal of water from hotplate-heated samples of Wiemann, Fabbri [58] likely promoted condensation reactions between biomolecules[59], enhancing AGE and ALE formation. Drying of tissues during maturation experiments are not realistically representative of typical burial environments preserving keratinous integumentary structures[60] (i.e., extensively waterlogged, reducing lacustrine or marine settings). In contrast, the use of a pressurised setup in this study inhibits water from boiling off, instead directing proteins along hydrolytic reaction pathways.

PCA further supports this position. The sulphur content of extracted melanin originates from benzothiazole moieties of phaeomelanin[19] whereas that of sediment-matured samples could derive from phaeomelanin, unleached keratin breakdown products, or from melanoidin-like polymers[58]. PC3 explains 9.86 % of the variation in the dataset **(Supplementary Fig. S4 a, b, c).** S-bearing fragments have a net positive loading on PC3 of either ~2.47 or ~2.22, depending on the ambiguous identity of the negatively loading fragment with m/z = ~134. The only S-bearing fragment(s) with negative loading on PC3 is/are large (containing six carbons and a nitrogen), possibly indicating incorporation within a larger polymer through thermal alteration, while the S-bearing fragments with positive loading on PC3 are typically smaller, possibly indicating that they are susceptible to volatilisation and loss through thermal alteration. Similar PC3 scores are observed across samples, but with slightly higher values in the sediment-matured feathers relative to the unmatured and capsule-matured melanin extracts as well as the fossils. There may also be a decrease in PC3 values as temperature increases in sediment maturation, consistent with the loss of volatile S-moieties, but sample sizes are small. The enrichment of presumably more volatile S-bearing moieties in the sediment-matured feathers could be indicative of unleached keratin breakdown products[28] (e.g., hydrolysed peptide fragments or free/degraded amino acids) due to (a) a lack of a decay treatment to reduce protein concentrations prior to maturation or (b) maturation in dry sediment, limiting dissolution of protein breakdown products. S-bearing fragments in sediment-matured feathers could also come from melanoidin-like polymers formed through maturation[58], again due to high protein and lipid concentrations when no decay has occurred prior to maturation or dry sediment that might favour condensation reactions. Regardless, this minor discrepancy in PC3 scores is not solely influenced by S-bearing fragments, used here as a proxy (albeit imperfect due to phaeomelanin confounding) for keratin-derived molecules, and would at most explain <10% of the variation in the data. Therefore, we can confidently say that any protein products or melanoidin-like polymers in sediment-matured samples are in very low quantities (consistent with observed volume loss in the impressions) and that PCA mostly describes variation in melanin chemistry. Similar PC3 scores between fossils and melanin extracts further highlight that protein loss is natural during fossilisation.

Sediment-encased P/T maturation elucidates melanin diagenesis

Animal integumentary structures (e.g., skin, scales, feathers, and hair) are composed of organic mixtures[63] of proteins, lipids (e.g., waxes/oils), and pigments. When integumentary structures undergo fossilisation, complex organics proceed through multiple steps. Comparison of experimental results with fossils in terms of appearance and chemistry suggests that experimental maturation of feathers results in thermobaric decomposition of organics. We hypothesise that, like natural diagenesis, P/T-maturation favours hydrolytic loss of integumentary proteins – evidenced by significant volume loss leading to voids/impressions as noted in prior work[28, 30].

Lipids, such as waxes and triglycerides, are predicted to undergo thermally mediated hydrolytic cleavage of ester bonds (e.g., between hydrophobic fatty acids and hydrophilic glycerol/glycerol phosphate groups[64]). After hydrolysis, severed hydrocarbon chains can undergo *in situ* polymerisation to be retained within fossils as insoluble aliphatic hydrocarbons (i.e. kerogen)[25, 65]. PCA distinguishes fossils from modern and experimental (capsule- and sediment-matured) samples. Lower PC2 values in modern/experimental samples compared to fossils are driven largely by enrichment in hydrocarbons (C_xH_y-), possibly originating from residual fatty acids and labile lipids (e.g., epidermal oils/waxes or melanosome lipid bilayers) in the modern/experimental samples that are depleted in fossils **(Supplementary Fig. S5 a, b)**. Labile lipid hydrocarbons could have been lost from fossils during post-mortem peroxidation (i.e., early stage decay) and/or through prolonged late stage oxidative weathering of kerogen.

Melanin pigments are thought to have linear heteropolymeric, stacked oligomeric structures, or combination of both[66], and have been shown to be resistant to hydrolysis except under harsh alkaline or acidic conditions[67, 68]. Multiple lines of evidence suggest that increasing PC1 scores correlate with increasing P/T alteration consistent with diagenesis: (1) At fixed pressure, PC1 scores increase with increasing maturation temperature; (2) open systems are shifted to higher PC1 scores; (3) non-hydrocarbon, especially N-bearing, fragments heavily load PC1 (e.g., C_xS_y-, C_xH_yS-, C_xN-, C_xH_yN-, C_xNS-, C_xNO-, C_xNSO-) **(Fig. 3a)**, where certain smaller fragments (i.e., volatiles) have negative loading while large fragments (i.e., components of polymers) have positive loading.

When fragment masses were plotted against PC1 loading (**Fig. 3b**), large fragments had strong positive loading whereas certain small fragments had strong negative loadings, suggesting that these small volatiles are progressively lost during maturation whereas larger moieties are enriched at higher temperatures through polymerisation. Unmatured melanin extract with the lowest PC1 scores are the least altered and enriched in only certain small fragments. Capsule-matured melanin extracts have lower PC1 scores compared to sediment-matured feathers at the same temperature, most likely because they are enriched in those small fragments (i.e., the closed system traps volatiles/labile products otherwise lost in open-system sediment). These

observations agree with previously published trends[13, 31] and suggest that loss of certain volatile/labile moieties concurrent with polymerisation/crosslinking occurs during melanin diagenesis, especially with respect to heteroatomic compounds such as N/S-bearing compounds.

We hypothesise that melanin undergoes thermal decomposition in several overlapping steps (i.e. volatile loss and polymerisation are overlapping at certain temperatures, but different processes are dominant at different temperatures). First, certain volatile/labile N/S/O-bearing compounds are lost as evidenced by smaller to larger secondary ion mass with both increased maturation temperature and increased system openness. Next, thermal crosslinking of eumelanin monomers (i.e., dihydroxyindoles and dihydroxyindole carboxylic acids) and oligomerisation of phaeomelanin benzothiazole units are expected occur[54, 68, 69]. We infer this in our experiments from the dark stains left on the bentonite matrix (~190–225°C).

Finally, significant thermal decomposition of melanin (i.e., chemical /alteration of the polymer) occurs at higher temperatures leading to carbonisation/charring followed by decarbonisation/oxidation around 300°C for eumelanin and maybe even lower (e.g., closer to 250°C) for phaeomelanin. In sediment-matured feathers, phaeomelanin-dominated samples (i.e., reddish-brown and grey) start to show signs of stain fading at ~250°C, whereas eumelanin-dominated samples (i.e., black and iridescent) do so by ~300°C. PCA shows very high thermal alteration and enrichment of polymers at ~250°C followed by reversal towards the PC1 origin at ~300°C, consistent with increased carbonisation/charring followed by decarbonisation/oxidation, leading first to carbon-rich then organic-depleted samples **(Fig. 2 a, b)**.

We posit that black and iridescent feather stains can survive harsher temperature regimes compared to brown and grey feathers. The observations of (a) stain retention at higher temperatures, (b) possible trends in PC1 scores according to melanin colour within each treatment/sample category, and (c) apparent reversal of this pattern at ~300°C suggest that that eumelanin has higher diagenetic stability than phaeomelanin. Seemingly intermediate positions occupied by mixed/organ melanin and grey colours along PC1 would suggest an intermediate composition and maturation stability, consistent with other studies[70, 71].

Future work

The ultimate goal of maturation setups is to simulate natural diagenesis in the laboratory. The expected result would produce matured tissues that are structurally and chemically comparable to carbonaceous compression fossils. While our current setup closely mimics the macroscopic staining and key aspects of diagenetic chemical signatures, compaction and P/T-maturation are temporally decoupled. The original orientation of melanosome layers in specimens (e.g. in structurally iridescent arrays) can be altered through the current setup[28]. To minimise this, future setups should compact and mature specimens concurrently.

Additionally, this study compares previously published capsule-maturation of enzymatically extracted melanin to sediment-encased maturation of whole feathers with pigments, proteins, lipids, etc., so the effect of greater chemical complexity in the whole tissues of fossils and sediment-matured samples should be further controlled in future work. Although, as noted above, there is good evidence that these ToF-SIMS signatures are driven primarily by melanin rather than keratin protein (for comparisons of raw spectra see **Supplementary Fig. S2**). Chemical variation between modern/experimental samples and fossils is most possibly due to lipid loss during early decay or late oxidative weathering. This can be potentially accounted for in future experimental designs through the addition of pre-maturation decay treatments or by subjecting samples to oxidation after maturation using warm, moist, oxygenated air.

Lastly, temperature can fluctuate by ~2–5 °C inside the sample chamber of the current maturation rig, albeit of minimal concern when examining samples across a 300°C temperature range. Temperature gradients are more noticeable with scaling up to larger sample chambers. Future improvements in chamber design should help to minimise temperature fluctuations and produce samples that are even more similar to natural fossils.

Materials And Methods

Sample Collection

Mass spectra of (1) freshly extracted melanin, (2) closed-system capsule-matured extracted melanin, and (3) fossilised melanin were obtained from Colleary, Dolocan [13], Clements, Dolocan [31] to compare with our sediment-encased maturation of feather sub-samples. Samples from pennaraptoran dinosaurs *Yi qi* STM 31-2 and *Sapeornis* STM 15-18 were collected from the Shandong Tianyu Museum of Nature in Pingyi, China. Naturally shed feathers (black, iridescent, brown, and grey) were collected from UK-based poultry farms, the Royal Society for Prevention of Cruelty to Animals (RSPCA) West Hatch Animal Centre in Taunton, UK, and the Hong Kong Zoological and Botanical gardens and Hong Kong Society for Prevention of Cruelty to Animals in China. No animals were harmed in acquiring feather samples and the samples were collected in accordance with Schedule 1 of the United Kingdom Animals (Scientific Procedures) Act (1986) and Section 15, Wild Animals Protection Ordinance, Agriculture, Fisheries and Conservation Department (AFCD), Hong Kong. For further details on specimens/samples, see **Supplementary Table S1**.

Hydraulic Compaction

Sediment-encased P/T maturation comprises two phases: (1) hydraulic compaction of the sample within sediment and (2) self-regulating P/T maturation. Our method and equipment are modified from those of Saitta, Kaye [28] (**Fig. 4**). Samples are compacted within sediment using a modified Perkin-Elmer tablet die press (**Fig. 4a**) consisting of upper and lower interlocking halves, a metal plunger, a metal sealing disc, a sediment tapper (not figured), and a spacer ring. The die press components are first cleaned with 70% ethanol and cotton swabs to remove remaining grit, ensuring a tight seal while preventing jamming of the plunger. The upper half of the die press is inverted, and the spacer ring is first placed around it. The metal plunger and the

plastic plunger are subsequently fed through the channel of the die press, leaving enough space to load the sample and surrounding Ca^{2+}-bentonite clay (purchased from ClayTerra, Wyoming, USA; https:/clayterra.com/). Approximately half the total amount of the clay is loaded into the channel and levelled with the smooth side of the sediment tapper. Feathers were either cut into small pieces or clipped with a hole puncher to select only the region of the feather with the colour of interest. The feather fragment is placed onto the surface of the clay layer, the remaining half of clay is then loaded over the sample and the sealing disc is loaded into the channel. A post-maturation split line can be induced by placing foil between the sample and remaining half of the clay prior to compaction to ensure even splitting of the tablet, and this was used on only four samples in the study **(Supplementary Table S1;** Samples 58, 59, 76, and 77**)**. The lower half of the die press is then united with the top half, and the whole compaction unit is placed under a hydraulic press that drives the metal plunger into the channel, compressing the sediment with a force of 8 tonnes over an area of 126.7 mm^2. Afterward, the upper and lower halves of the die press are separated, the spacer ring is placed between them, and the hydraulic press is used to push the clay tablet out of the channel.

Self-regulated P/T maturation

Maturation equipment (**Fig. 4b**) consisted of an insulated metal pipe with an AC-powered heating rod or AC-powered resistor coil. Some initial low temperature runs were conducted using a heating rod in contact with the sample chamber, but these failed when attempting temperatures greater than 200°C. The setup was subsequently improved by instead using a resistive coil to attain higher temperatures. Both heaters are directly comparable, given the homeostatic temperature control system. The tablets were loaded into a smaller metal sample holder (~19 mm diameter) positioned inside the larger insulated pipe and attached to a K-type thermocouple temperature sensor. The high-pressure airline connected a Shoebox air compressor to the larger metal pipe. Once the pressure inside the pipe reached ~70% of the final pressure, the heater was turned on and the temperature was calibrated by adjusting the output voltage on the transformer unit. When the final pressure of 250 bars was attained, the temperature and pressure within the metal pipe were maintained in an automated fashion using a digital feedback controller unit connected to the pressure gauge and the shoebox air-compressor. Maturation was performed on compacted clay tablets encasing feather samples at ~190°C (190–193°C), ~200 °C (200–202°C), ~225°C (225–229°C), ~250°C (250–252°C), and ~300°C (300–305°C) with a pressure of 250 bars for 24 hrs. After each maturation run, the setup was allowed to cool down first and then depressurised. Then, the smaller sample holder and thermocouple temperature sensor were taken out of the metal pipe, and tablets were recovered and glued on their external clay surfaces to aluminium electron microscopy stubs with cyanoacrylate. Finally, most of the pellets were split after maturation by wedging a razor blade, while a few that unevenly split were further prepped by hand tools (e.g., dental pick).

ToF-SIMS

The ToF-SIMS parameters chosen were comparable to that of previous work on fossil, modern, and experimental melanin in order for us to combine our data with previously published datasets [13, 31, 33]. An ION-TOF ToF-SIMS V (located at the Materials Characterisation and Preparation Facility, Hong Kong University of Science and Technology, Hong Kong SAR, China) was used. The setup used a pulsed (18 ns, 10 kHz) primary ion beam consisting of Bi_3^+ clusters at 30-kV ion energy with low-energy electron flooding for charge compensation. The rationale for choosing polyatomic sputtering (i.e., Bi_3^+ clusters) was to improve the signal by reducing fragmentation of large organic molecules and to be consistent with previous ToF-SIMS data collection[13]. Data of high mass resolution was acquired in bunched mode (~5000 m/Δm, spatial resolution ~0.2–0.3 mm) for experimental and fossil samples (acquired from barbs/barbules in the case of feathers). The ion beam was scanned over areas ranging between 50–500 mm^2 at 256 pixels for each sample. The base pressure during spectra acquisition was <1 Å, or ~10^{-8} mbar. Mass calibration of ion peaks was conducted by identifying C-cluster peaks from C_1–C_9. Previously published spectra for melanin reported 55 characteristic negative secondary ion peaks[13, 60], and these were used in our analysis. These peaks were normalised based on total-ion m/z counts for a given spectrum and mean-centred using the formula: $-\Sigma(\text{ion count}_i - \mu_{\text{ion count}})$. Normalised and mean-centred peak data then underwent PCA using JMP 14.0 software.

Declarations

Author Contributions

A.R., M.P., T.G.K., and E.T.S. designed the research. A.R., M.P., T.G.K., and E.T.S. provided samples/new tools/infrastructure for research. T.G.K. built the experimental rig based on a design by T.G.K. and E.T.S. A.R. and E.T.S. performed statistical analyses on the data. A.R., M.P., E.T.S. and T.G.K. wrote the paper.

Acknowledgments

We thank Caitlin Colleary (Cleveland Museum of Natural History, Cleveland, OH, USA) for sharing ToF-SIMS data of fossils as well as data of fresh and capsule-matured melanin extract. We also thank Akiko Shinya (Field Museum of Natural History, Chicago, IL, USA) for her assistance in preparing a few of the sediment-encased maturation samples that did not initially split cleanly. We thank Jakob Vinther (University of Bristol, Bristol, United Kingdom) for assistance in obtaining feather samples, discussion on feather maturation experimentation, and for his collaboration that led to the first-generation setup reported by Saitta, Kaye [28]. Kind thanks to Peter Sjövall, RISE Research Institutes of Sweden, Borås, Sweden for providing us a reference β-keratin ToF-SIMS spectra from Schweitzer, Zheng [56]. We would also like to thank Lu-Tao Weng (Materials Characterisation and Preparation Facility, Hong Kong University of Science and Technology) for running ToF-SIMS on our samples, Xiaoli Wang and Xiaoting Zheng (Shandong Tianyu Museum of Nature, Pingyi, China; Institute of Geology and Paleontology, Linyi University, China) for fossil feather samples from the pennaraptoran dinosaurs *Yi qi* STM 31-2 and *Sapeornis* STM 15-18 housed at Shandong Tianyu Museum of Nature.

References

1. Slater TS, McNamara ME, Orr PJ, Foley TB, Ito S, Wakamatsu K. Taphonomic experiments resolve controls on the preservation of melanosomes and keratinous tissues in feathers. *Palaeontology* **63**, 103-115 (2020).

2. McNamara ME*, et al.* Non-integumentary melanosomes can bias reconstructions of the colours of fossil vertebrates. *Nat Commun* **9**, 2878 (2018).

3. McNamara ME, Briggs DE, Orr PJ, Field DJ, Wang Z. Experimental maturation of feathers: implications for reconstructions of fossil feather colour. *Biology Letters* **9**, 20130184 (2013).

4. McNamara ME, Orr PJ, Kearns SL, Alcala L, Anadon P, Molla EP. Soft-Tissue Preservation in Miocene Frogs from Libros, Spain: Insights into the Genesis of Decay Microenvironments. *Palaios* **24**, 104-117 (2009).

5. Vinther J, Briggs DE, Prum RO, Saranathan V. The colour of fossil feathers. *Biology Letters* **4**, 522-525 (2008).

6. Li Q*, et al.* Plumage color patterns of an extinct dinosaur. *Science* **327**, 1369-1372 (2010).

7. Hu DY*, et al.* A bony-crested Jurassic dinosaur with evidence of iridescent plumage highlights complexity in early paravian evolution. *Nat Commun* **9**, 12 (2018).

8. Wang X*, et al.* Basal paravian functional anatomy illuminated by high-detail body outline. *Nat Commun* **8**, 14576 (2017).

9. Briggs DE, Moore RA, Shultz JW, Schweigert G. Mineralization of soft-part anatomy and invading microbes in the horseshoe crab Mesolimulus from the Upper Jurassic Lagerstatte of Nusplingen, Germany. *Proc Biol Sci* **272**, 627-632 (2005).

10. Parry LA, Wilson P, Sykes D, Edgecombe GD, Vinther J. A new fireworm (Amphinomidae) from the Cretaceous of Lebanon identified from three-dimensionally preserved myoanatomy. *BMC Evol Biol* **15**, 256 (2015).

11. Rossi V, McNamara ME, Webb SM, Ito S, Wakamatsu K. Tissue-specific geometry and chemistry of modern and fossilized melanosomes reveal internal anatomy of extinct vertebrates. *Proceedings of the National Academy of Sciences*, 201820285 (2019).

12. Gabbott SE, Donoghue PC, Sansom RS, Vinther J, Dolocan A, Purnell MA. Pigmented anatomy in Carboniferous cyclostomes and the evolution of the vertebrate eye. *Proceedings of the Royal Society of London B: Biological Sciences* **283**, 20161151 (2016).

13. Colleary C*, et al.* Chemical, experimental, and morphological evidence for diagenetically altered melanin in exceptionally preserved fossils. *Proceedings of the National Academy of Sciences USA* **112**, 12592-12597 (2015).

14. Manning PL*, et al.* Pheomelanin pigment remnants mapped in fossils of an extinct mammal. *Nat Commun* **10**, 2250 (2019).

15. Raff EC*, et al.* Embryo fossilization is a biological process mediated by microbial biofilms. *Proc Natl Acad Sci U S A* **105**, 19360-19365 (2008).

16. Purnell MA*, et al.* Experimental analysis of soft-tissue fossilization: opening the black box. *Palaeontology* **61**, 317-323 (2018).

17. Briggs DE, Summons RE. Ancient biomolecules: their origins, fossilization, and role in revealing the history of life. *Bioessays* **36**, 482-490 (2014).

18. Sansom RS, Gabbott SE, Purnell MA. Atlas of vertebrate decay: a visual and taphonomic guide to fossil interpretation. *Palaeontology* **56**, 457-474 (2013).

19. Roy A, Pittman M, Saitta ET, Kaye TG, Xu X. Recent advances in amniote palaeocolour reconstruction and a framework for future research. *Biol Rev Camb Philos Soc* **95**, 22-50 (2019).

20. Bath Enright OG, Minter NJ, Sumner EJ. Palaeoecological implications of the preservation potential of soft-bodied organisms in sediment-density flows: testing turbulent waters. *Royal Society open science* **4**, 170212 (2017).

21. Voorhies MR. Taphonomy and population dynamics of an early Pliocene vertebrate fauna, Knox County, Nebraska. *Rocky Mountain Geology* **8**, 1-69 (1969).

22. Behrensmeyer AK. Time resolution in fluvial vertebrate assemblages. *Paleobiology*, 211-227 (1982).

23. Moyer AE*, et al.* Melanosomes or microbes: testing an alternative hypothesis for the origin of microbodies in fossil feathers. *Scientific Reports* **4**, 4233 (2014).

24. Allison PA. The role of anoxia in the decay and mineralization of proteinaceous macro-fossils. *Paleobiology*, 139-154 (1988).

25. Gupta NS, Cody GD, Tetlie OE, Briggs DE, Summons RE. Rapid incorporation of lipids into macromolecules during experimental decay of invertebrates: initiation of geopolymer formation. *Organic Geochemistry* **40**, 589-594 (2009).

26. Glass K*, et al.* Impact of diagenesis and maturation on the survival of eumelanin in the fossil record. *Organic Geochemistry* **64**, 29-37 (2013).

27. Briggs DEG. The role of decay and mineralization in the preservation of soft-bodied fossils. *Annual Review of Earth and Planetary Sciences* **31**, 275-301 (2003).

28. Saitta ET, Kaye TG, Vinther J. Sediment-encased maturation: a novel method for simulating diagenesis in organic fossil preservation. *Palaeontology*, (2018).

29. Saitta ET*, et al.* Low fossilization potential of keratin protein revealed by experimental taphonomy. *Palaeontology* **60**, 547-556 (2017).

30. Saitta ET, Vinther J. A perspective on the evidence for keratin protein preservation in fossils: An issue of replication versus validation. (2019).

31. Clements T, Dolocan A, Martin P, Purnell MA, Vinther J, Gabbott SE. The eyes of Tullimonstrum reveal a vertebrate affinity. *Nature* **532**, 500-503 (2016).

32. Lindgren J, Caldwell MW, Konishi T, Chiappe LM. Convergent evolution in aquatic tetrapods: insights from an exceptional fossil mosasaur. *PLoS One* **5**, e11998 (2010).

33. Lindgren J, *et al.* Skin pigmentation provides evidence of convergent melanism in extinct marine reptiles. *Nature* **506**, 484-488 (2014).

34. Lindgren J, *et al.* Soft-tissue evidence for homeothermy and crypsis in a Jurassic ichthyosaur. *Nature* **564**, 359 (2018).

35. Hong L, Garguilo J, Anzaldi L, Edwards GS, Nemanich RJ, Simon JD. Age-dependent photoionization thresholds of melanosomes and lipofuscin isolated from human retinal pigment epithelium cells. *Photochemistry and Photobiology* **82**, 1475-1481 (2006).

36. Liu Y, *et al.* Comparison of Structural and Chemical Properties of Black and Red Human Hair Melanosomes. *Journal of Photochemistry and Photobiology* **81**, 135-144 (2005).

37. Saitta ET, *et al.* Preservation of feather fibers from the Late Cretaceous dinosaur Shuvuuia deserti raises concern about immunohistochemical analyses on fossils. *Organic Geochemistry* **125**, 142-151 (2018).

38. Nordén KK, *et al.* Melanosome diversity and convergence in the evolution of iridescent avian feathers—Implications for paleocolor reconstruction. *Evolution*, (2018).

39. Li Q, *et al.* Reconstruction of Microraptor and the evolution of iridescent plumage. *Science* **335**, 1215-1219 (2012).

40. Glass K, *et al.* Direct chemical evidence for eumelanin pigment from the Jurassic period. *Proceedings of the National Academy of Sciences USA* **109**, 10218-10223 (2012).

41. Littke R, Rotzal H, Leythaeuser D, Baker D. Lower Toarcian Posidonia Shale in southern Germany (Schwäbische Alb). Organic facies, depositional environment, and maturity. *Erdöl und Kohle, Erdgas, Petrochemie vereinigt mit Brennstoff-Chemie* **44**, 407-414 (1991).

42. Prauss M, Ligouis B, Luterbacher H. Organic matter and palynomorphs in the 'Posidonienschiefer'(Toarcian, Lower Jurassic) of southern Germany. *Geological Society, London, Special Publications* **58**, 335-351 (1991).

43. Marshall CP, Mar GL, Nicoll RS, Wilson MA. Organic geochemistry of artificially matured conodonts. *Organic Geochemistry* **32**, 1055-1071 (2001).

44. Michels R, Landais P. Artificial coalification: comparison of confined pyrolysis and hydrous pyrolysis. *Fuel* **73**, 1691-1696 (1994).

45. Kaye TG, Pittman M, Mayr G, Schwarz D, Xu X. Detection of lost calamus challenges identity of isolated Archaeopteryx feather. *Scientific Reports* **9**, 1182 (2019).

46. Zhang F*, et al.* Fossilized melanosomes and the colour of Cretaceous dinosaurs and birds. *Nature* **463**, 1075-1078 (2010).

47. Smithwick FM, Nicholls R, Cuthill IC, Vinther J. Countershading and Stripes in the Theropod Dinosaur Sinosauropteryx Reveal Heterogeneous Habitats in the Early Cretaceous Jehol Biota. *Curr Biol* **27**, 3337-+ (2017).

48. Carney RM, Vinther J, Shawkey MD, D'Alba L, Ackermann J. New evidence on the colour and nature of the isolated Archaeopteryx feather. *Nat Commun* **3**, 637 (2012).

49. de Souza Carvalho I, Novas FE, Agnolín FL, Isasi MP, Freitas FI, Andrade JA. A Mesozoic bird from Gondwana preserving feathers. *Nat Commun* **6**, 1-5 (2015).

50. Kundrát M*, et al.* A polar dinosaur feather assemblage from Australia. *Gondwana Research* **80**, 1-11 (2020).

51. Thomas DB, Nascimbene PC, Dove CJ, Grimaldi DA, James HF. Seeking carotenoid pigments in amber-preserved fossil feathers. *Scientific Reports* **4**, 5226 (2014).

52. Field DJ, D'Alba L, Vinther J, Webb SM, Gearty W, Shawkey MD. Melanin concentration gradients in modern and fossil feathers. *PLoS One* **8**, e59451 (2013).

53. Vitek NS, Vinther J, Schiffbauer JD, Briggs DE, Prum RO. Exceptional three-dimensional preservation and coloration of an originally iridescent fossil feather from the Middle Eocene Messel Oil Shale. *Paläontologische Zeitschrift* **87**, 493-503 (2013).

54. Vinther J. Reconstructing Vertebrate Paleocolor. *Annual Review of Earth and Planetary Sciences* **48**, 345-375 (2020).

55. Cincotta A*, et al.* Chemical preservation of tail feathers from Anchiornis huxleyi, a theropod dinosaur from the Tiaojishan Formation (Upper Jurassic, China). *Palaeontology* **n/a**.

56. Schweitzer MH, Zheng W, Moyer AE, Sjövall P, Lindgren J. Preservation potential of keratin in deep time. *PloS one* **13**, e0206569 (2018).

57. Wiemann J, Crawford JM, Briggs DEG. Phylogenetic and physiological signals in metazoan fossil biomolecules. *Science Advances* **6**, eaba6883 (2020).

58. Wiemann J*, et al.* Fossilization transforms vertebrate hard tissue proteins into N-heterocyclic polymers. *Nat Commun* **9**, 4741 (2018).

59. Hodge JE. Dehydrated foods, chemistry of browning reactions in model systems. *Journal of agricultural and food chemistry* **1**, 928-943 (1953).

60. Saitta E, Vinther J. A perspective on the evidence for keratin protein preservation in fossils: An issue of replication versus validation. *Palaeontologia Electronica*, (2019).

61. Alleon J, Montagnac G, Reynard B, Brule T, Thoury M, Gueriau P. Pushing Raman spectroscopy over the edge: purported signatures of organic molecules in fossils are instrumental artefacts. *bioRxiv*, 2020.2011.2009.375212 (2020).

62. Wiemann J, Yang T-R, Norell MA. Dinosaur egg colour had a single evolutionary origin. *Nature*, (2018).

63. Morrison ML, Rodewald AD, Voelker G, Colón MR, Prather JF. *Ornithology: Foundation, Analysis, and Application*. JHU Press (2018).

64. Eglinton G, Logan GA. Molecular preservation. *Philos Trans R Soc Lond B Biol Sci* **333**, 315-327; discussion 327-318 (1991).

65. Stankiewicz BA, Hutchins JC, Thomson R, Briggs DE, Evershed RP. Assessment of bog-body tissue preservation by pyrolysis-gas chromatography/mass spectrometry. *Rapid Commun Mass Spectrom* **11**, 1884-1890 (1997).

66. Watt AAR, Bothma JP, Meredith P. The supramolecular structure of melanin. *Soft Matter* **5**, 3754-3760 (2009).

67. Ito S, Nakanishi Y, Valenzuela RK, Brilliant MH, Kolbe L, Wakamatsu K. Usefulness of alkaline hydrogen peroxide oxidation to analyze eumelanin and pheomelanin in various tissue samples: application to chemical analysis of human hair melanins. *Pigment Cell & Melanoma Research* **24**, 605-613 (2011).

68. Ito S, Wakamatsu K, Glass K, Simon JD. High-performance liquid chromatography estimation of cross-linking of dihydroxyindole moiety in eumelanin. *Analytical biochemistry* **434**, 221-225 (2013).

69. Greco G, Panzella L, Verotta L, d'Ischia M, Napolitano A. Uncovering the structure of human red hair pheomelanin: benzothiazolylthiazinodihydroisoquinolines as key building blocks. *Journal of Natural Products* **74**, 675-682 (2011).

70. Liu SY, Shawkey MD, Parkinson D, Troy TP, Ahmed M. Elucidation of the chemical composition of avian melanin. *RSC Advances* **4**, 40396-40399 (2014).

71. McGraw KJ, Wakamatsu K, Clark AB, Yasukawa K. Red-winged blackbirds Agelaius phoeniceus use carotenoid and melanin pigments to color their epaulets. *Journal of Avian Biology* **35**, 543-550 (2004).

Figures

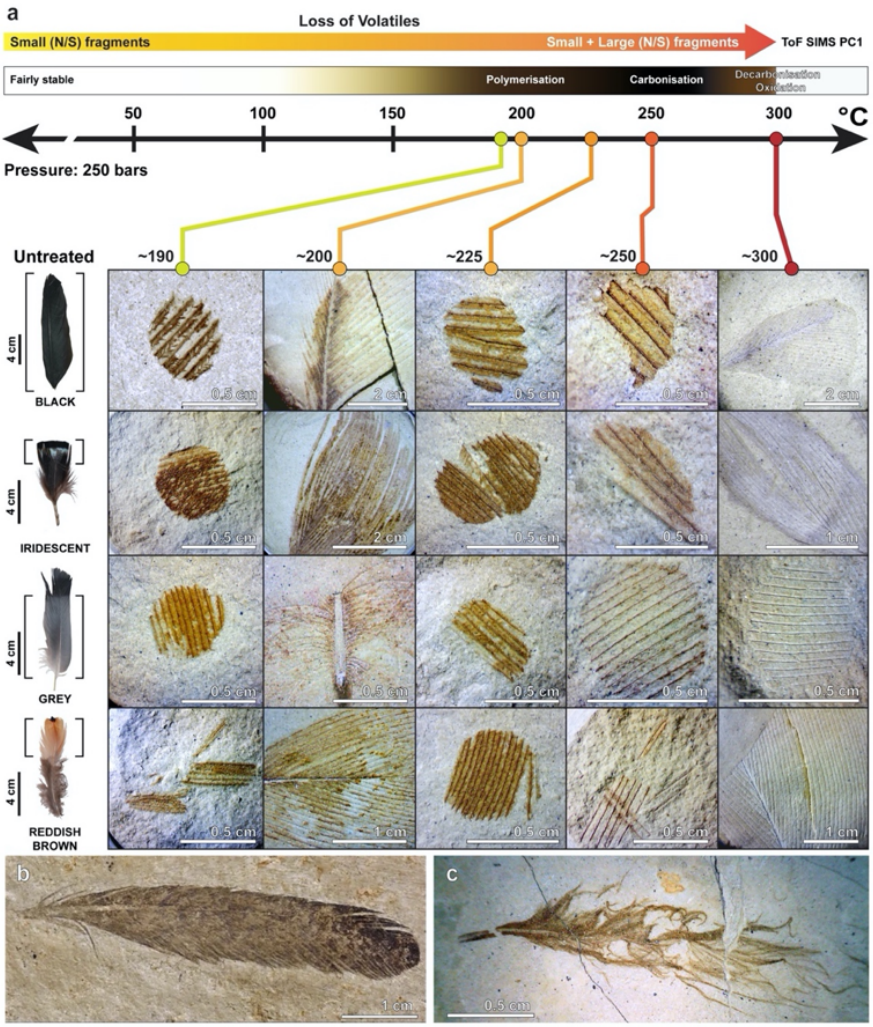

Figure 1

Physical appearance of organic staining in sediment-matured samples matches that of exceptionally preserved fossil feathers. Feather sub-samples were cut or hole-punched from coloured regions designated by brackets. a Changes in colour of organic stains occur during maturation. Original colour shown for untreated feathers in the left column and different temperature categories shown to the right, revealing brown organic stains in the clay matrix. Based on stain patterns and organic chemistry from ToF-SIMS, we predict that diverse melanic colours converge upon brown stains due to crosslinking/polymerisation of melanin in the experimental temperature range of ~190–225°C, coinciding with volatile loss. Increased charring/carbonisation of the molecule likely occurs when approaching ~250°C followed by decarbonisation/oxidation (i.e., complete loss of organic carbon in the form of CO2) when approaching ~300°C. b Isolated pennaraptoran feather (MB.Av.100) from the Late Jurassic Solnhofen Limestone45 and c isolated pennaraptoran feather (IVPP V15388B)46 from the Early Cretaceous Jehol Group.

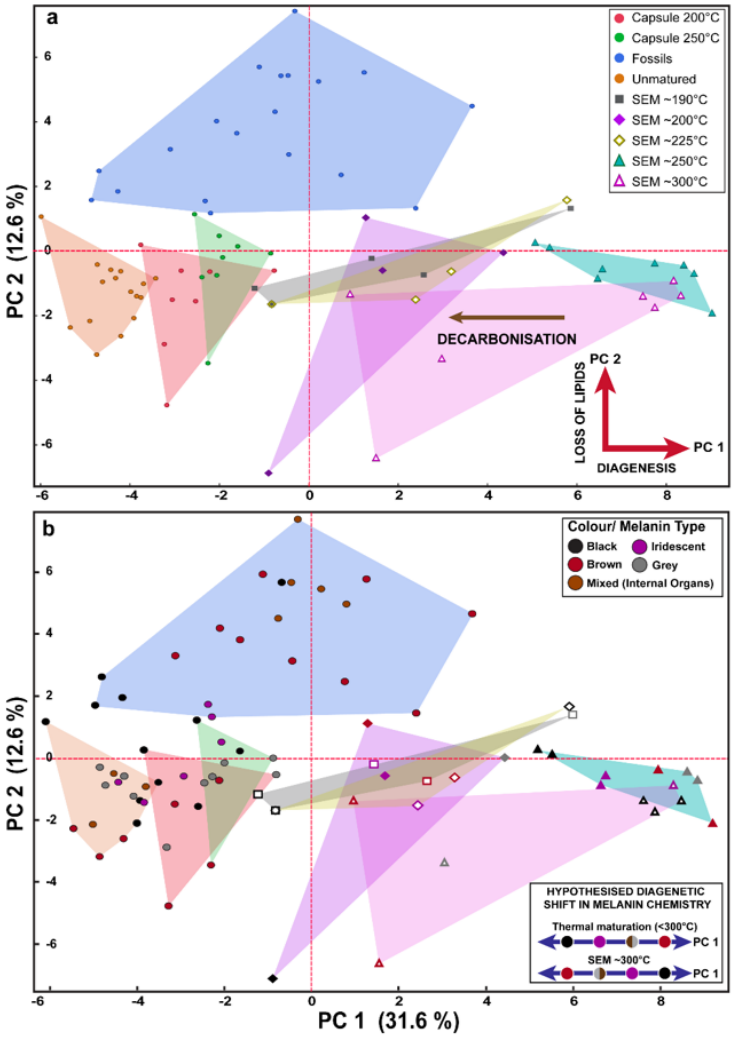

Figure 2

PCA on ToF-SIMS data of fossil and experimental samples. a Comparison of secondary ion spectra of fresh melanin extracts, capsule-matured melanin extracts, sediment-encased maturation (SEM) of whole feathers, and fossil samples. Experimental samples sort along PC1 which describes the P/T maturation/diagenetic continuum. Sediment matured samples at ~300°C appear to show a reversal towards decreasing PC1, indicating decarbonisation. For a more detailed PCA with data points descriptions see Supplementary Table 1 and Supplementary Fig. S1a. b Same PCA as in a, but melanin type/colour produced for each sample is indicated. Based on PC1 loadings within each sample category, we hypothesise different susceptibility to diagenetic alteration across the colour categories from most to least stable: black, iridescent, mixed visceral organ melanin/grey (i.e., intermediate compositions of eu- and phaeomelanin), and brown. ~300°C sediment-matured samples are hypothesised to show a reversal of this pattern in PC1 values, whereby phaeomelanin decarbonises most readily while eumelanin shows more stability.

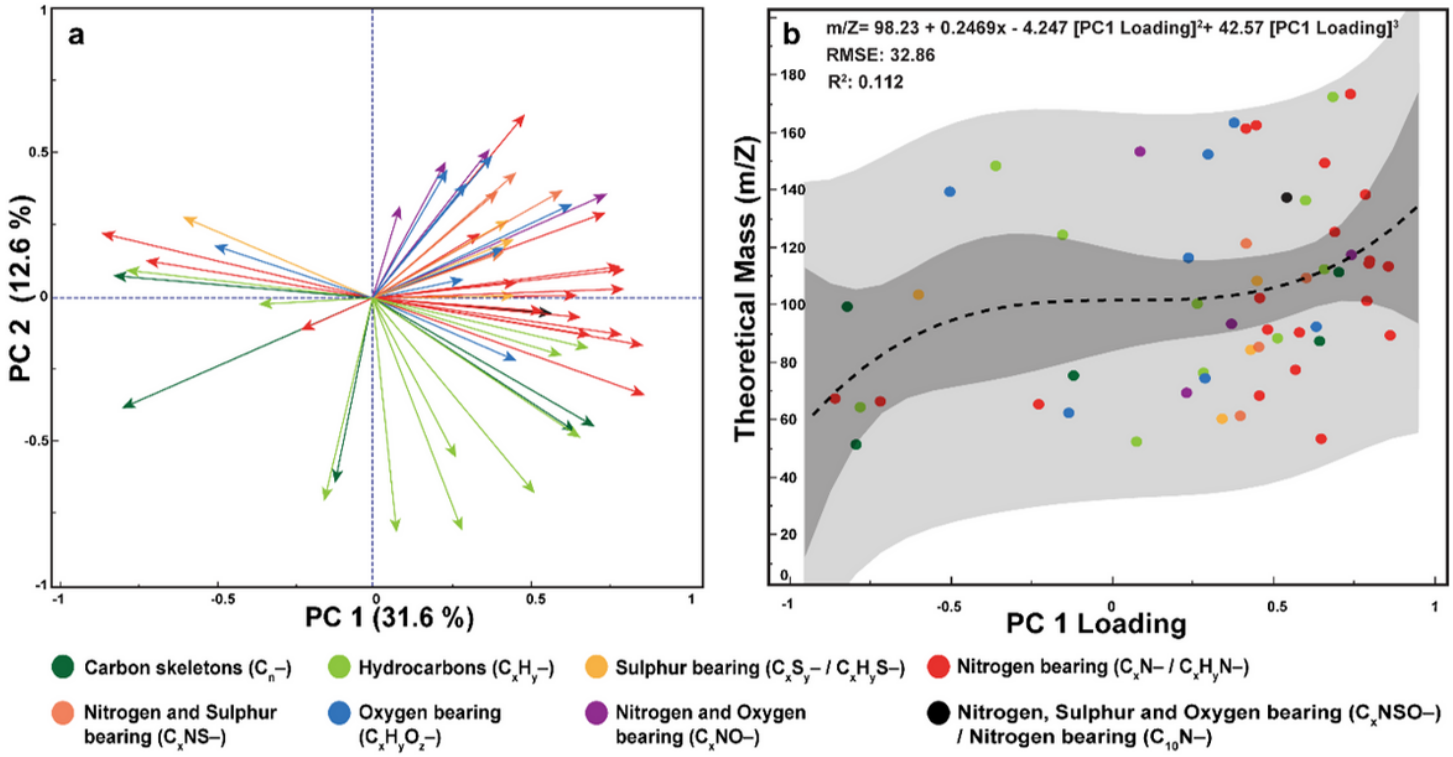

Figure 3

a Loading plot indicating the relative contributions of secondary ion fragments on PC1 and PC2. The black arrow indicates an ambiguous fragment that is either CxNSO- (m/Z 134.00) or C10N- (m/Z 133.97). For a more detailed PCA loading plot with chemical fragment descriptions see Supplementary Table S2 and Supplementary Fig. S1b. b Plot of theoretical mass of secondary ion fragments against their PC1 loadings indicating that certain fragments with smaller masses are enriched at lower temperatures and closed systems (i.e., negative PC1 loadings), whereas these fragments become depleted at higher temperatures and open systems. Fragments with higher masses tend to have higher/positive PC1 loadings. This suggests a progressive loss of small, volatile organics under higher temperatures and sediment pore filtration, while more recalcitrant organics polymerise/crosslink. Capsule maturation likely traps volatiles normally lost in sediment-encased maturation.

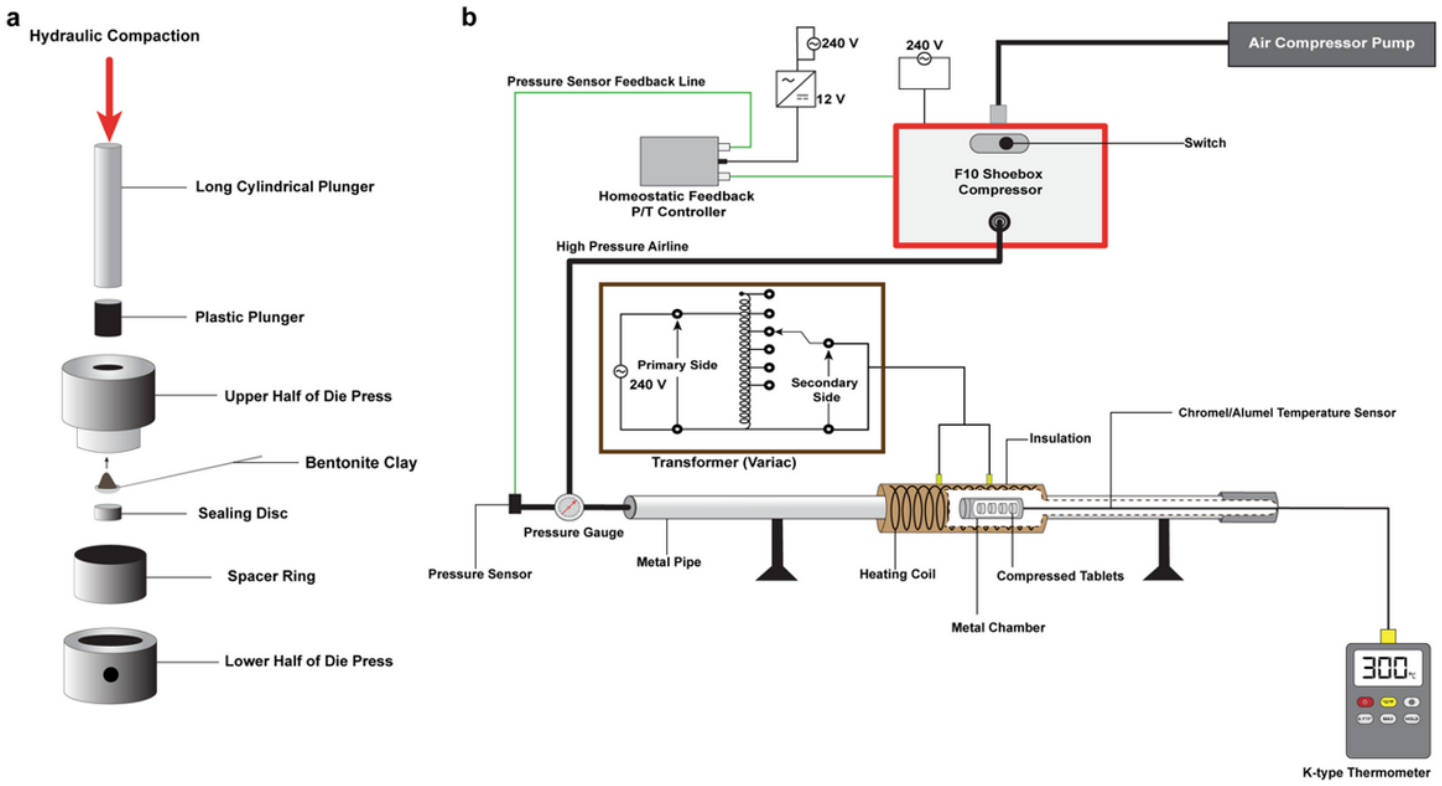

Figure 4

Two-part next-generation experimental setup a Die press for compaction of samples in sediment. b Schematic diagram of the P/T maturation rig shown with heating coil setup.

Supplementary Files

This is a list of supplementary files associated with this preprint. Click to download.

- RoyetalSedimentencasedpressuretemperaturematurationexperimentschemicallysimulatenaturaldiagenesisofmelaninSupplementaryInformation.docx
- RoyetalTOFSIMSPCAworksheet.xlsx